




ORIGINAL RESEARCH

Improving estimation performance of compressive sensing-based multiple-input multiple-output radar using electronic beamsteering

 Max Schurwanz¹  | Jan Mietzner²  | Peter Adam Hoher¹ 
¹Kiel University (CAU), Kiel, Germany²Hamburg University of Applied Sciences (HAW), Hamburg, Germany**Correspondence**Max Schurwanz.
Email: masc@tf.uni-kiel.de**Funding information**

German Federal Ministry of Economic Affairs and Climate Action, Grant/Award Number: 20D1905B

Abstract

Two-dimensional direction-of-arrival (DoA) estimation in azimuth and elevation via radar systems equipped with uniform rectangular arrays (URAs) will play an important role in various application areas—most distinctively in future urban air mobility settings with unmanned aerial vehicles. A key factor is the fast and reliable provision of target detections in terms of range and DoA for safe autonomous operation of the vehicle using on-board antenna arrays with compact installation size. The authors present a technique for improving the performance of DoA estimation using compressive sensing in conjunction with multiple-input multiple-output arrays with electronically steered beams in the transmit direction. The simulation study investigates the impact of different design considerations on radar signal processing performance. An optimisation of a radar system using electronic beamsteering in the transmit domain is presented numerically. Based on the architecture of the URAs used, performance and detection accuracy can be improved.

1 | INTRODUCTION

Radar systems have been an integral part of surveillance and monitoring for over a century, beginning with the first use to detect ships in poor visibility and for early-warning and fire-control tasks in World War II. Today, the use of electromagnetic waves to detect the presence, position, and velocity of objects is used extensively for searching, tracking, and imaging purposes [1]. With a general trend in aviation towards urban air mobility (UAM) with small and more flexible air vehicles that are capable of automatic- and vertical takeoff and landing (ATOL/VTOL), reliable and compact automatic sensing systems are required for safe operation [2]. At the same time, unmanned aerial vehicle (UAV), autonomous aerial vehicle (AAV), or remotely piloted aircraft system (RPAS) platforms offer only limited installation space, calling for small-size, low-weight, and also energy-efficient sensor solutions. Radar sensors are attractive, due to their all-weather and day-and-night capability.

With multi-antenna systems, the design of such antenna arrays can be exploited to enable further features and improve

on the tradeoff between precision and cost [3]. Multiple-input multiple-output (MIMO) radar systems have attracted a lot of attention over recent years [4]. Antenna apertures can be virtually increased by utilising orthogonal signals at the transmitter side [5]. This results in higher resolution and better accuracy in the angular domain while allowing for a compact installation size [6]. Separating antennas in the spatial domain also increases the resolution of estimated target parameters like range, angle, and velocity [7].

Conventional phased array radars use coherent radio frequency phase shifters at each antenna element to steer the array's main lobe in a preferred direction using beamforming (BF) techniques [8]. This enables the use of beamformed energy as opposed to a (mostly uniform) energy distribution achieved by single antenna elements and their angular characteristics. Using this coherent feeding technique, the array gain pattern can be shaped to suppress sidelobes or optimise energy into a preferred direction [9]. Array pattern shaping has been applied to radar sensor arrays to optimise the direction-of-arrival (DoA) estimation results, for example, in [10–15]. Contrary to phased arrays, studies using subarray partitioning

This is an open access article under the terms of the [Creative Commons Attribution](https://creativecommons.org/licenses/by/4.0/) License, which permits use, distribution and reproduction in any medium, provided the original work is properly cited.

© 2024 The Authors. *IET Radar, Sonar & Navigation* published by John Wiley & Sons Ltd on behalf of The Institution of Engineering and Technology.

and combining such techniques with MIMO arrays have shown that the angular resolution can be improved significantly [16–20].

Radar signal processing employs appropriate algorithms to estimate a target's range, velocity, and position [21, 22]. Estimating the DoA of a reflected signal at the receiving sensor array can be a challenging task. This is especially true when simultaneously determining the velocity and range of the target. Nonetheless, it holds significant importance in dynamic scenarios. An exemplary UAM scenario is illustrated in Figure 1. Each AAV, UAV, or RPAS has to sense and predict the movement of surrounding platforms and obstacles in a detect and avoid fashion.

Conventional spectral-based BF methods or subspace-based methods such as MULTIPLE SIGNAL CLASSIFICATION [23] or ESTIMATION OF SIGNAL PARAMETERS VIA ROTATIONAL INVARIANT TECHNIQUES (ESPRIT) [24] rely on the statistical information of the received signal and therefore require a certain amount of received data to form a statistically significant spatial covariance matrix [25]. The energy in the covariance matrix can be searched for targets in the angular domain to obtain an arbitrarily accurate DoA estimation. The resolution can in theory be improved by increasing the number of received samples, that is, the integration time, to form a more significant covariance matrix.

Considering highly dynamic scenarios in UAM with multiple UAVs in close proximity, the primary goal is to increase the update interval. This could ultimately be achieved by reducing the number of samples required for DoA estimation. A promising way to use fewer samples while achieving high accuracy is provided by the concept of compressive sensing (CS), which is a class of techniques able to solve

underdetermined systems of linear equations with sparse inputs [26–28]. CS has been applied to many different domains in radar signal processing [29], for example, to reconstruct sparse signals with sampling rates far below the Nyquist-rate [30, 31], for DoA estimation [32, 33], array design [34], and extended target detection [35]. In terms of hardware design, it has been shown that CS performs well with pseudo-random array topologies [34, 36] and also with widely separated antenna arrays with inter-element spacing $d > \lambda$ [37, 38]. The most important requirement to apply CS to a scenario is sparsity of the latter in relation to the systems basis. Most UAM scenarios can be assumed sparse when discriminating the present targets in the range and velocity domain (prior to DoA estimation). This means that only very few targets are simultaneously present in the same range-Doppler cell. In such cases, an exhaustive search over the entire FoV, for example, based on conventional digital beamforming (DBF) on receive combined with an appropriate energy detection algorithm, like constant false alarm rate (CFAR), would be inefficient. Instead of this, CS can output binary results representing the position of a target in azimuth and elevation.

Additionally, in many aviation scenarios, one angular dimension is of more interest than the other and requires a higher resolution. This might happen in flight route planning when relying on horizontal flight manoeuvres only. In this case the azimuth position of a target is much more important than its elevation, which can be estimated rather coarsely. In typical UAM scenarios, however, depending on prevailing flight trajectories, three-dimensional (3D) situational awareness (in range, azimuth, and elevation) is required. An implementation with separate processing of the two angular domains in azimuth and elevation offers the possibility to perform faster calculations and generate different angular accuracies—adapted to the respective requirements of the flight manoeuvres [14]. The additional possibility of reducing the physical size and thus the weight of the antenna arrays by means of a MIMO radar approach represents one of the most important requirements for use in aviation.

1.1 | Contributions, related work, and outline

This paper investigates the use of electronic beamsteering on the transmitter side of MIMO radars with two-dimensional arrays to steer the main lobe of the array simultaneously in azimuth and elevation. It is combined with CS algorithms on the receiver side to estimate the DoA in sparse target scenarios. This simple codebook-based electronic beamsteering approach via analogue or digital phase shifters is compared to conventional MIMO signal processing employing a wide illumination to establish the virtual antenna array. Related papers in the area of applying CS to DoA estimation with MIMO antenna arrays utilise a-priori DoA information to optimise digital BF at the receiver [39]. They address optimisation of receiver side combining and degrees of freedom for sparse antenna arrays [40], and improve on compressive sampling to reduce the

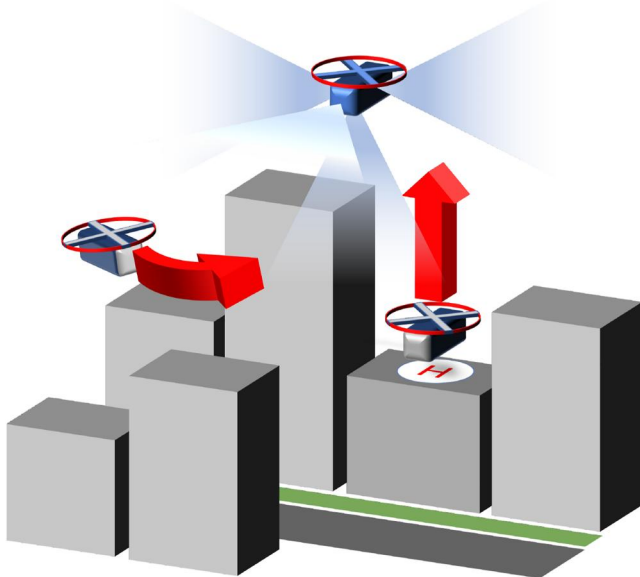


FIGURE 1 Highly dynamic urban air mobility (UAM) example scenario with three unmanned aerial vehicles (UAVs) in an urban environment. The field-of-view (FoV) of the radar arrays of the hovering UAV is illustrated by the blue cones.

number of RF-chains at the receiver [41]. This work focuses on the design of specific electronic transmit beamsteering sets for MIMO arrays, without a-priori target DoA information, and investigates effects on the resulting accuracy of CS-based DoA estimation.

A normalisation scheme, previously applied to a one-dimensionally steered array in [14], is extended to two-dimensional beamsteering to keep a fair comparison between MIMO signal processing arrays and electronic beamsteering. While MIMO arrays are limited in a way, as the number of antenna elements and orthogonal signals restrict the size of the virtual aperture, electronic beamsteering opens up further degrees of freedom to signal processing. Two-dimensional beamsteering also increases its benefits in conjunction with CS signal processing on the receiver side.

The main contributions of this paper are as follows:

- For the considered application, we propose to employ 2D-MIMO arrays in a novel fashion, by moving from the common virtual array processing to a beamsteering mode of operation for improved performance of CS-based DoA estimation.
- To this end, the system model from ref. [14] is extended to account for two-dimensional electronic transmit beamsteering in azimuth and elevation.
- The extended system model enables the analysis and optimisation of this two-dimensional domain in DoA estimation using CS algorithms. In particular this optimisation is applied and tailored to the requirements of future UAM scenarios, which involve fast and reliable target detection in range, azimuth, and elevation.
- A relation between the selected beamsteering directions and the result of the DoA estimation process based on numerical evaluations of the sensing matrix is presented using its Gramian representation.
- Based on the results, design recommendations for the creation of suitable beamsteering sets based on an existing antenna layout or, conversely, an antenna layout with a corresponding beamsteering set, are given.

This simulative study illustrates the advantage of a separated processing of the azimuth and elevation domain for DoA estimation, previously introduced in ref. [14]. In contrast to previous studies on transmit BF-based DoA estimation [16, 19, 20], this paper examines the impact of a deliberate choice of beamsteering directions in the form of an offline beamsteering codebook on the reconstruction performance of CS algorithms. In particular, our scheme does not require any prior information, as opposed to refs. [17, 18]. These works use subarray partitioning to form a hybrid phased-MIMO radar system capable of coherently integrating the received signals and optimising the beam pattern. Furthermore, our work only considers electronic beamsteering based on phase-shifters, whereas other works such as [10, 11] employ orthogonal signals based beam pattern synthesis to achieve a given wideband pattern. Our scheme thus only steers the main lobe of the transmit antenna array. Based on

this, design considerations leading to the most promising approach are presented and evaluated for practical use cases, based on the more comprehensive measure of the Gramian matrix.

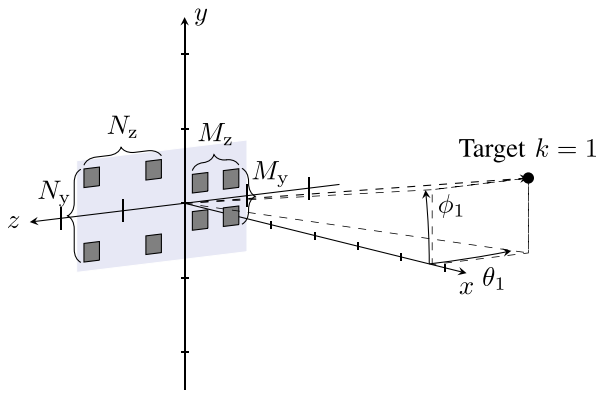
The remainder of this paper is organised as follows: Section 2 introduces the general system model of the antenna array which can be used for both conventional MIMO signal processing and electronic beamsteering modes, which are described in detail in Section 3. Section 4 presents the applied CS-based DoA estimation method. Section 5 gives an overview of the different scenarios and antenna topologies investigated and presents corresponding simulation results. In Section 6, the effects of antenna design considerations on the overall performance with both signal processing modes are discussed, before a conclusion is drawn in Section 7.

1.2 | Mathematical notation

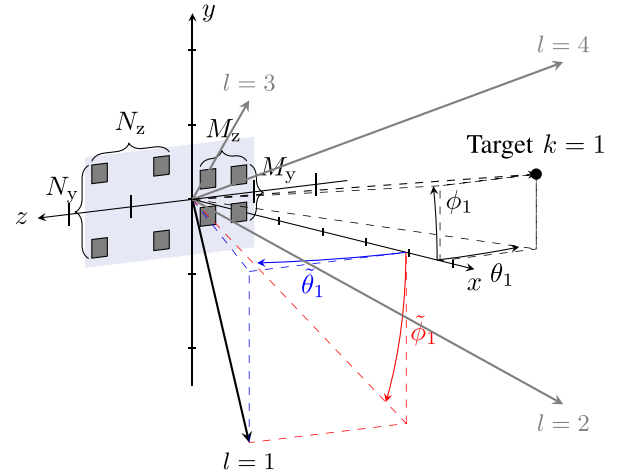
Throughout this paper, vectors and matrices are presented as bold-face lower-case and upper-case characters \mathbf{x} and \mathbf{X} , respectively. The i th entry of a vector is denoted as x_i and the entry in the i th row and j th column of a matrix is written as x_{ij} . The i th column of a matrix \mathbf{X} is referred to as \mathbf{X}_i . Furthermore, $(\cdot)^T$ is the matrix transpose operator, $(\cdot)^H$ is the conjugate transpose operator, $(\cdot)^*$ is the complex conjugate operator, and $\text{vec}(\mathbf{X})$ is the column-wise vectorisation of a matrix \mathbf{X} . The flooring operation is denoted by $\lfloor \cdot \rfloor$, where the operand is rounded down to the next smaller integer number. $\mathbf{1}_N$ denotes a column vector of length N with unity entries, and $\mathbf{0}_N$ denotes a corresponding vector with zero entries. Finally, $j = \sqrt{-1}$ denotes the imaginary unit.

2 | SYSTEM MODEL

The radar system described in this paper consists of two uniform rectangular arrays (URAs) for transmit and receive operation placed in the yz -plane with boresight direction in x -direction. The number of elements in each dimension is given by (M_y, M_z) for the transmit array and (N_y, N_z) for the receive array. Figure 2 illustrates the example $M_y = M_z = N_y = N_z = 2$. The case where the transmit and receive arrays are restricted to a single dimension (e.g. $M_z = N_y = 1$ or $M_y = N_z = 1$) describes the special case of a simple MIMO array with transmit steering capability in only one dimension (cf. [14]). For 2D MIMO arrays, the distance between the elements of either the transmit or the receive array must be increased to ensure an optimal virtual aperture in the sense of a minimum redundancy array design. For electronic beamsteering, the transmit elements must be spaced at most $\lambda/2$ apart to avoid generating grating lobes in the FoV. Correspondingly, when the spacing of the receive elements is increased the MIMO array is able to support both a MIMO virtual antenna and an electronic



(a) Orthogonal signals from all transmit elements ensure that the signals can be recovered at the receiver via matched filtering for MIMO signal processing.



(b) Simplest case of two-dimensional array geometry capable of steering the main lobe of the transmit array in azimuth and elevation direction θ_1 and ϕ_1 , respectively. In this example, a 2×2 steering set is used.

FIGURE 2 Example array with two 2×2 transmit and receive arrays. For illustration purposes, the transmit and receive arrays were spatially displaced along the z -axis, which is not necessary for a working implementation. The arrays could also be nested within one another (for a more compact installation) while still achieving the same virtual aperture.

beamsteering mode. (In the simple one-dimensional case, this issue does not need to be considered [14], as the linear transmit and receive arrays are arranged in a perpendicular fashion.) Both arrays employ uniform spacing between the array elements given by the variables $(d_{Tx,y}, d_{Tx,z})$ and $(d_{Rx,y}, d_{Rx,z})$ normalised to the centre wavelength λ_c of the radar system. The wavelength is given by $\lambda_c = c_0/f_c$, with f_c representing the centre frequency of the radar system and c_0 the speed of light. In the MIMO case the transmit array defines the spacing of the receive array to maximise the virtual aperture, which results in $d_{Rx,y} = M_y d_{Tx,y}$ and $d_{Rx,z} = M_z d_{Tx,z}$. Throughout the paper, this MIMO setup is taken as the basic URA configuration.

Furthermore, we adopt the following assumptions from [34]:

- We employ the far-field approximation with planar wavefronts being assumed at the antenna arrays. This implies that the target range has to meet a corresponding lower limit. Given a radar system operating at 10 GHz and using a relatively large antenna aperture, far field already starts within the range of a few metres. Furthermore, this range becomes even smaller with increasing frequency and/or smaller apertures. Correspondingly, the far-field assumption is valid for typical UAM scenarios and practicable target ranges.
- All targets are assumed to only occupy a single range-Doppler cell for simplicity (point-target assumption).
- Clutter is neglected, as it is assumed to be fully separable from targets by means of Doppler filtering, and noise in the system is assumed to be additive white Gaussian noise (AWGN).

The processing chain within the radar system after the analog radar frontend follows a conventional model shown in ([34], Figure 1), where the raw data is range-compressed before

a filtering step in the Doppler domain. The energy in the range-Doppler domain is then filtered, and spatial processing in the form of DoA estimates is performed using the CS algorithm presented in Section B.

The array elements are numbered column-wise via linear indices $m = 1, 2, \dots, M_y \cdot M_z$ for the transmit array and $n = 1, 2, \dots, N_y \cdot N_z$ for the receive array. This results in the definition of the array positions in y - and z -dimension (cf. Figure 2), given as

$$y_{Tx,m} = \lambda_c d_{Tx} \cdot \left((m - 1 \bmod M_y) - \frac{M_y - 1}{2} \right) \quad (1)$$

$$z_{Tx,m} = \lambda_c d_{Tx} \cdot \left(\frac{m - 1}{M_y} - \frac{M_z - 1}{2} \right)$$

for the transmit array and

$$y_{Rx,n} = \lambda_c d_{Rx} \cdot \left((n - 1 \bmod N_y) - \frac{N_y - 1}{2} \right) \quad (2)$$

$$z_{Rx,n} = \lambda_c d_{Rx} \cdot \left(\frac{n - 1}{N_y} - \frac{N_z - 1}{2} \right)$$

for the receive array. Following [32, 34], the radar scenario describes K targets with radar cross-section values σ_k , ranges from the radar array given by r_k , and angular coordinates given by (θ_k, ϕ_k) in terms of azimuth and elevation.

A general formula to calculate the phase difference at an antenna element with offset d related to the phase centre ($y = 0, z = 0$) of the array, given an angle of departure/arrival η (defined within the (x, y) -plane/ (x, z) -plane w.r.t. the x -axis) is given by

$$\zeta(d, \eta) = \frac{2\pi d}{\lambda_c} \sin \eta. \quad (3)$$

The transmit steering factor corresponding to the m th transmit element and the k th target thus is given by the following:

$$t_m(\theta_k, \phi_k) = \exp(j[\zeta(y_{Tx,m}, \phi_k) + \zeta(z_{Tx,m}, \theta_k)]). \quad (4)$$

The receive steering factor at the n th receive element from the k th target is given in the same way by

$$r_n(\theta_k, \phi_k) = \exp(j[\zeta(y_{Rx,n}, \phi_k) + \zeta(z_{Rx,n}, \theta_k)]). \quad (5)$$

From these factors, the transmit and receive steering vectors $\mathbf{t}(\theta_k, \phi_k) \in \mathbb{C}^{M_x M_y}$ and $\mathbf{r}(\theta_k, \phi_k) \in \mathbb{C}^{N_x N_y}$ pointing in the direction of the azimuth and elevation angle θ_k and ϕ_k of the k th target are defined as follows:

$$\mathbf{t}(\theta_k, \phi_k) = [t_1(\theta_k, \phi_k) \quad \dots \quad t_{M_x M_y}(\theta_k, \phi_k)]^T, \quad (6)$$

and

$$\mathbf{r}(\theta_k, \phi_k) = [r_1(\theta_k, \phi_k) \quad \dots \quad r_{N_x N_y}(\theta_k, \phi_k)]^T. \quad (7)$$

Finally, τ_k represents the two-way propagation delay between the radar and the k th target.

3 | RADAR MODES

In the sequel, the considered radar modes used in comparison are discussed in detail. Both modes employ the same physical antenna array for transmit and receive operation but differ in the nature of transmitted and received waveforms.

3.1 | Multiple-input multiple-output signal processing

MIMO signal processing utilises orthogonal transmit signals, which can be optimally separated at the receiver using time-domain matched filtering. This creates a virtual aperture at the spatial convolutions of the individual transmit and receive antenna element positions increasing the aperture from $M_x M_y + N_x N_y$ physical elements to a theoretical maximum of $M_x M_y N_x N_y$ virtual elements, given appropriate element placement and sufficiently many mutually orthogonal signals. An example antenna configuration with two URAs is presented in Figure 2a.

The vector $\mathbf{s}(t) = [s_1(t), \dots, s_{M_x M_y}(t)]^T$ describes $M_y \cdot M_x$ orthogonal unit-power transmit signals. Following [32], the receive vector $\mathbf{y}_{\text{MIMO}} \in \mathbb{C}^{M_x M_y N_x N_y}$ is given by the matched filter output in ref. (8), where the second equality holds for the case of perfect signal orthogonality.

$$\begin{aligned} \mathbf{y}_{\text{MIMO}} &= \text{vec} \left(\int \mathbf{s}(t - \tau_k) \mathbf{s}^H(t - \tau_k) t \sum_{k=1}^K \mathbf{t}(\theta_k, \phi_k) \mathbf{r}^T(\theta_k, \phi_k) \sigma_k \right) \\ &= \text{vec} \left(\sum_{k=1}^K \mathbf{t}(\theta_k, \phi_k) \mathbf{r}^T(\theta_k, \phi_k) \sigma_k \right) \end{aligned} \quad (8)$$

3.2 | Electronic beamsteering signal processing

In electronic beamsteering, all transmitting antennas use the same coherent signal $s(t)$ and are active simultaneously [42]. By means of (analog and/or digital) phase shifters, the main lobe of the array is steered in a predefined direction in azimuth $\tilde{\theta}_l$ and elevation $\tilde{\phi}_l$. At the receiver, this primary direction can be recovered from the received signal by means of time-domain matched filtering with respect to the transmit signal $s(t)$. In this way the transmitted signal can also be optimally reconstructed here. Beamsteering offers the possibility to increase the number of degrees of freedom for estimating the DoA of impinging signals without increasing the number of transmit and receive antennas. With a two-dimensional transmit array geometry, a beamsteering in both azimuth and elevation direction is possible, which enables a more focused beam.

The main lobe of the transmit array is subsequently steered into L individual directions, defined in azimuth and elevation

$$(\tilde{\theta}_l, \tilde{\phi}_l) \in \{(\tilde{\theta}_1, \tilde{\phi}_1), \dots, (\tilde{\theta}_L, \tilde{\phi}_L)\}, \quad (9)$$

as illustrated in Figure 2b for four particular directions ($l = 1, \dots, 4$), by employing corresponding phase shifts at the individual transmit elements. The phase shift v applied to the transmit signal at the m th transmit element is calculated as follows:

$$\begin{aligned} v_m(\tilde{\theta}_l, \tilde{\phi}_l) &= \frac{1}{L} \exp(-j[\zeta(y_{Tx,m}, \tilde{\phi}_l) + \zeta(z_{Tx,m}, \tilde{\theta}_l)]), \\ m &= 1, 2, \dots, M_y \cdot M_x, \end{aligned} \quad (10)$$

which results in the definition of the transmit steering vector corresponding to the l th steering direction, which is applied to all transmit elements simultaneously:

$$\mathbf{v}(\tilde{\theta}_l, \tilde{\phi}_l) = [v_1(\tilde{\theta}_l, \tilde{\phi}_l) \quad \dots \quad v_{M_x M_y}(\tilde{\theta}_l, \tilde{\phi}_l)]^T. \quad (11)$$

The received signal after steering the transmit beam subsequently into all steering directions is defined as a vector $\mathbf{y}_{\text{steer}} \in \mathbb{C}^{L N_x N_y}$, capturing the summation of the echos from all targets $k = 1, \dots, K$ after matched filtering at the receiver. It is given by Equation (12). Note that we perform electronic beamsteering only at the transmitter side, because the resulting measurement matrix has a better condition (see numerical results).

$$\mathbf{y}_{\text{steer}} = \begin{bmatrix} \sum_{k=1}^K \mathbf{v}^T(\tilde{\theta}_1, \tilde{\phi}_1) [\mathbf{t}(\theta_k, \phi_k) \mathbf{r}^T(\theta_k, \phi_k)]^T \sigma_k \int s^*(t - \tau_k) s(t - \tau_k) t \\ \vdots \\ \sum_{k=1}^K \mathbf{v}^T(\tilde{\theta}_l, \tilde{\phi}_l) [\mathbf{t}(\theta_k, \phi_k) \mathbf{r}^T(\theta_k, \phi_k)]^T \sigma_k \int s^*(t - \tau_k) s(t - \tau_k) t \\ \vdots \\ \sum_{k=1}^K \mathbf{v}^T(\tilde{\theta}_L, \tilde{\phi}_L) [\mathbf{t}(\theta_k, \phi_k) \mathbf{r}^T(\theta_k, \phi_k)]^T \sigma_k \int s^*(t - \tau_k) s(t - \tau_k) t \end{bmatrix} = \begin{bmatrix} \sum_{k=1}^K [\mathbf{r}(\theta_k, \phi_k) \mathbf{t}^T(\theta_k, \phi_k)] \mathbf{v}(\tilde{\theta}_1, \tilde{\phi}_1) \sigma_k \\ \vdots \\ \sum_{k=1}^K [\mathbf{r}(\theta_k, \phi_k) \mathbf{t}^T(\theta_k, \phi_k)] \mathbf{v}(\tilde{\theta}_l, \tilde{\phi}_l) \sigma_k \\ \vdots \\ \sum_{k=1}^K [\mathbf{r}(\theta_k, \phi_k) \mathbf{t}^T(\theta_k, \phi_k)] \mathbf{v}(\tilde{\theta}_L, \tilde{\phi}_L) \sigma_k \end{bmatrix} \quad (12)$$

A visual representation of the effect of electronic transmit beamsteering can be obtained by the transmit array factor which can be calculated via

$$\text{AF}_{\text{Tx}}(\theta, \phi) = \mathbf{v}^T(\tilde{\theta}_l, \tilde{\phi}_l) \mathbf{t}(\theta, \phi), \quad (13)$$

or the full (transmit and receive) array factor

$$\text{AF}(\theta, \phi) = \mathbf{v}^T(\tilde{\theta}_l, \tilde{\phi}_l) [\mathbf{t}(\theta, \phi) \mathbf{r}^T(\theta, \phi)]^T, \quad (14)$$

for an angular direction given by (θ, ϕ) . Exemplary normalised array factors are presented in Figure 3 for four different steering directions in azimuth and elevation. Notice that the electronic beamsteering set is clearly visible in Figure 3a which shows the array factor of the transmitting array. The receive array performing no BF at all simply spreads the received energy over azimuth and elevation which is not useful for illustrating purposes as shown based on the full array factor in Figure 3b.

4 | CS BASED DIRECTION-OF-ARRIVAL ESTIMATION TECHNIQUE

This paper investigates the possibilities for performance improvement of an electronically steered two-dimensional MIMO array using CS as a DoA estimation technique. CS as a mathematical discipline for solving underdetermined linear systems of equations can, under certain conditions, provide an advantage in sparse scenarios and achieve good DoA estimates with few measured values. As stated in the introduction, UAM radar scenarios are known to be mostly sparse, as the targets can—in a first processing step—be discriminated into individual range-Doppler cells. Thus, DoA estimation presents a perfect domain to utilise the capabilities of CS. Furthermore, if an initial target detection step is employed after range-Doppler processing, for example, via a 2D CFAR algorithm, CS DoA estimation may be confined to range-Doppler cells with an

active target detection. This limits the overall computational complexity.

In this work, we use iterative hard thresholding (IHT) [43] as the CS method of choice because this algorithm is quite simply implemented and can be parameterised to the expected number of targets within the FoV. Another possible algorithm to use would be orthogonal matching pursuit [44], among others. Both algorithms use an angular grid for DoA estimation. Correspondingly, a sensing matrix has to be defined based on which the angular positions of the targets are estimated.

4.1 | Sensing matrix construction

The entries in the sensing matrix are defined over a uniformly spaced grid in azimuth and elevation with spacings given by $\delta\theta$ and $\delta\phi$. As there are P grid points in azimuth and Q points in elevation, the grid is spanned by the two vectors.

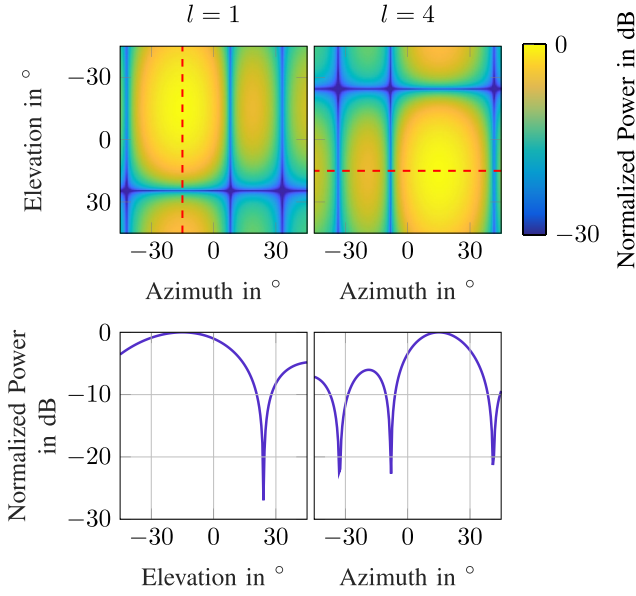
$$\boldsymbol{\theta} = \delta\theta \cdot \left([0, 1, \dots, (P-1)]^T - \frac{P-1}{2} \right), \quad (15)$$

$$\boldsymbol{\phi} = \delta\phi \cdot \left([0, 1, \dots, (Q-1)]^T - \frac{Q-1}{2} \right), \quad (16)$$

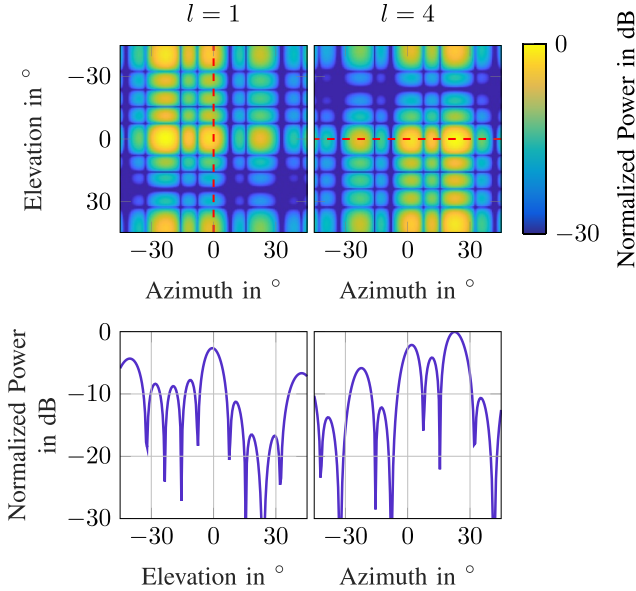
where P and Q are selected as odd numbers. This results in the formulation of an auxiliary dictionary Ψ to reference the grid points. This dictionary is defined as follows:

$$\Psi = \left[\text{vec}(\boldsymbol{\theta} \cdot \mathbf{1}_Q^T), \text{vec}(\mathbf{1}_P \cdot \boldsymbol{\phi}^T) \right]. \quad (17)$$

The sensing matrix entries are composed in a similar way as Equations (8) and (12) with the transmit and receive steering vectors defined over the discrete grid in azimuth and elevation with azimuth angles $\theta_i \in \boldsymbol{\theta}$ and elevation angles $\phi_i \in \boldsymbol{\phi}$. Considering the case of MIMO processing, with discrete grid defined in this way, a sensing matrix is obtained that examines



(a) Transmit array factor for $l = 1$ and $l = 4$ with exemplary elevation and azimuth array factor cuts (dashed red lines).



(b) Combined transmit and receive array factor for $l = 1$ and $l = 4$ with exemplary elevation and azimuth array factor cuts (dashed red lines).

FIGURE 3 Normalised power of array gain of an array layout with 15 transmit ($M_y = 3$, $M_z = 5$) and 15 receive antenna elements ($N_y = 5$, $N_z = 3$). As an example, transmit beamsteering is done in $L = 4$ discrete directions $(\tilde{\theta}_l, \tilde{\phi}_l) \in \{(-15^\circ, -15^\circ), (-15^\circ, 15^\circ), (15^\circ, -15^\circ), (15^\circ, 15^\circ)\}$.

targets at the predefined grid points, associated with weight vectors

$$\mathbf{a}_{\text{MIMO}}(\theta_i, \phi_i) = \text{vec}(\mathbf{t}(\theta_i, \phi_i) \mathbf{r}^T(\theta_i, \phi_i)). \quad (18)$$

Considering the electronic beamsteering directions given by their phase shift vectors (10), the weight vectors at the receiver in the electronic beamsteering case are defined as

$$\mathbf{a}_{\text{steer}}(\theta_i, \phi_i) = \begin{bmatrix} \text{vec}([\mathbf{r}(\theta_i, \phi_i) \mathbf{t}^T(\theta_i, \phi_i)] \mathbf{v}(\tilde{\theta}_1, \tilde{\phi}_1)) \\ \vdots \\ \text{vec}([\mathbf{r}(\theta_i, \phi_i) \mathbf{t}^T(\theta_i, \phi_i)] \mathbf{v}(\tilde{\theta}_l, \tilde{\phi}_l)) \\ \vdots \\ \text{vec}([\mathbf{r}(\theta_i, \phi_i) \mathbf{t}^T(\theta_i, \phi_i)] \mathbf{v}(\tilde{\theta}_L, \tilde{\phi}_L)) \end{bmatrix}. \quad (19)$$

In contrast to the discrete angles of the angular dictionary, the beamsteering angles can have arbitrary values, which depend only on the resolution of the phase shifters and must be known at the receiver. For a monostatic system, however, this circumstance does not pose a problem. Regardless of the employed radar signal processing mode (MIMO processing or beamsteering), the full sensing matrix consists of the horizontal concatenation of the weight vectors for all possible grid points

$$\mathbf{A} = [\mathbf{a}(\theta_1, \phi_1), \dots, \mathbf{a}(\theta_P, \phi_Q)], \quad (20)$$

with $\mathbf{a}(\theta, \phi) = \mathbf{a}_{\text{MIMO}}(\theta, \phi)$ for MIMO processing and $\mathbf{a}(\theta, \phi) = \mathbf{a}_{\text{steer}}(\theta, \phi)$ for electronic beamsteering. This results in a $\mathbb{C}^{M_y M_z N_y N_z \times PQ}$ matrix in the case of MIMO signal processing and $\mathbb{C}^{LN_y N_z \times PQ}$ in the case of electronic beamsteering.

Note that \mathbf{A} is a rectangular matrix with less rows than columns, leading to an underdetermined linear system of equations, under the assumption that the number of grid points, PQ , exceeds the number of received signals, $M_y M_z N_y N_z$ or $LN_y N_z$, respectively.

4.2 | Iterative hard thresholding algorithm

CS estimates the input $\tilde{\mathbf{x}}$ of the underdetermined linear system

$$\mathbf{y} = \mathbf{A} \tilde{\mathbf{x}} + \boldsymbol{\epsilon}, \quad (21)$$

which holds the position of the targets in the angular domain, based on the system output \mathbf{y} which is given by either the MIMO mode response \mathbf{y}_{MIMO} or the electronic beamsteering response $\mathbf{y}_{\text{steer}}$. Additional additive noise is introduced by the vector $\boldsymbol{\epsilon}$.

The IHT algorithm used in this paper delivers good results while being computationally inexpensive. It computes the approximated residual $\tilde{\mathbf{x}}^{(i+1)}$ in its i th iteration via

$$\tilde{\mathbf{x}}^{(i+1)} = \mathbb{H}(\tilde{\mathbf{x}}^{(i)} + \mathbf{A}^T(\mathbf{y} - \mathbf{A} \tilde{\mathbf{x}}^{(i)})). \quad (22)$$

In the first iteration, the approximated residual is initialised with $\tilde{\mathbf{x}}^{(1)} = \mathbf{0}_{PQ}$ and the hard thresholding operator is defined as

$$\mathbb{H}(x_l) := \begin{cases} x_l, & \text{if } |x_l| > \sqrt{K}, \\ 0, & \text{else.} \end{cases} \quad (23)$$

The parameter K which the algorithm uses to threshold the results represents the number of targets expected in the FoV of the antenna array. The algorithm estimates the most promising DoA in each iteration, thus K iterations are performed for each estimation step, where in each step a single DoA estimation is produced.

5 | NUMERICAL SIMULATION

In the following, the presented system model description from Section 2 is used for DoA estimation in radar-centric two-dimensional polar coordinates. The goal of the numerical simulations is to compare both radar operation modes from Section 3 using the common framework introduced in Section 4. The MIMO operation is performed assuming perfectly orthogonal transmit signals at each transmit antenna element, which results in the aforementioned maximisation of its virtual aperture. The electronic beamsteering operation employs the same array architecture as the MIMO operation and differentiates between five exemplary steering sets. Each of these sets contains $L = 25$ combined steering directions in azimuth and elevation which is given by the angular range in which the electronic beamsteering is performed. The five exemplary steering sets are chosen to cover all ranges between wide beamsteering over the entire FoV to very narrow beamsteering with small phase differences between the transmit antennas. A tunable variable is used to demonstrate the impact of the steering range on the reconstruction performance of an arbitrary scenario. Each steering set is named after the range of steering it covers: Steer- S_{\max} is given by $Z_{\text{az}} \times Z_{\text{el}}$ steering directions in azimuth and elevation with equidistant azimuth steering directions θ_i

$$\frac{-S_{\max}}{2} \leq \theta_i \leq \frac{S_{\max}}{2}, \quad i = 1, \dots, Z_{\text{az}} \quad (24)$$

and equidistant elevation steering directions ϕ_i

$$\frac{-S_{\max}}{2} \leq \phi_i \leq \frac{S_{\max}}{2}, \quad i = 1, \dots, Z_{\text{el}}. \quad (25)$$

The exemplary steering ranges in these sets are defined by $S_{\max} \in \{5^\circ, 15^\circ, 30^\circ, 45^\circ, 60^\circ\}$ with $Z_{\text{az}} = Z_{\text{el}} = 5$.

Monte Carlo simulations are run with 1000 different random target locations in the FoV for different signal-to-noise ratio (SNR) values. Assuming AWGN at the receiver, and 250 realisations per location in azimuth and elevation, this results in an error variance of $1/\sqrt{2.5 \times 10^5} = 2 \times 10^{-3}$. The stationary, point-like targets are considered to be in separate range-Doppler cells, such that a sparse scenario with $K = 1$ can be assumed. The FoV of the array in azimuth and elevation is defined as $\pm 45^\circ$ (with an assumed element gain of 6dBi) and the target positions are drawn randomly and uniformly from this interval. The grid in Equations (15) and (16) which defines the sensing matrix describes the searchable domain for the DoA estimation algorithm and consists of $P = Q = 91$ grid

points per direction spaced with $\delta\theta = \delta\phi = 1^\circ$ which results in a grid covering the entire FoV. Although this angular grid is quite coarse, it allows for a comparison between the different techniques and at the same time for an implementation on inexpensive, commercially available hardware. An improvement of the DoA estimation in terms of resolution can be achieved with a finer grid.

To compare the results of both processing modes, the SNR has to be adapted to account for additional processing gain. The simulations use a time-slotted model to calculate the additional SNR penalty for the electronic beamsteering mode. As an orthogonal signalling scheme, time-division multiplexing (TDM) is assumed in the MIMO case, and the beamsteering time slots are assumed to be equal in length to one TDM slot. The SNR penalty (in dB) for the beamsteering mode results as follows:

$$P_{\text{penalty}} = 10\log_{10}\left(\frac{L}{M_y M_z}\right), \quad (26)$$

and is applied to the received signal after matched-filtering. With this penalty¹ the SNR in dB for the beamsteering mode is defined as follows:

$$\text{SNR} = 10\log_{10}\left(\frac{P_s}{P_n}\right) + P_{\text{penalty}}. \quad (27)$$

Here, P_s represents the desired signal power at the receiver (including BF gains in the case of electronic beamsteering) and $P_n = N_0 \cdot B$, with noise spectral density and channel bandwidth N_0 and B , respectively. With this fair comparison scheme established, a common SNR can be used to assess the impact of different beamsteering sets on the DoA estimation performance.

DoA estimation is done separately in azimuth and elevation, which brings a time-benefit, as the residual in the IHT algorithm reduces from length PQ to only P or Q , depending on the angular domain. With this processing scheme, a more precise relation between the array geometry and its performance in a certain domain can be drawn. DoA estimation performance is evaluated by both the root-mean-square error (RMSE) and the probability that a scenario cannot be correctly reconstructed (*reconstruction error probability*). The RMSE is an error magnitude measure, which provides the ability to quantify the accuracy of the angle estimation of each algorithm. The (reconstruction) error probability, on the other hand, is a binary measure, which highlights cases of imperfect reconstruction of target scenarios.

As a baseline measure, the smallest two-dimensionally steerable array layout with $M_y = M_z = N_y = N_z = 2$ elements is used. Steering is performed in $L = 25$ steering directions uniformly distributed in azimuth and elevation given the assigned steering range S_{\max} . Given these parameters, the

¹Note that the SNR penalty for the beamforming mode is actually a gain, if $L < M_y \cdot M_z$.

MIMO mode results in a virtual aperture with $4 \cdot 4 = 16$ elements while the electronic beamsteering can utilise $25 \cdot 4 = 100$ receive paths, which is compensated via an SNR penalty of $P_{\text{penalty}} = 7.96$ dB for the beamsteering mode. Figure 4 illustrates the RMSE for the given configuration with one target within the FoV. With the exception of the Steer-5° case, which performs worse, the RMSE is the same in both radar modes. The corresponding resulting error probability is shown in Figure 5. It can be noted that the electronic beamsteering mode performs as good as the MIMO mode, while it is even possible to slightly outperform the orthogonal

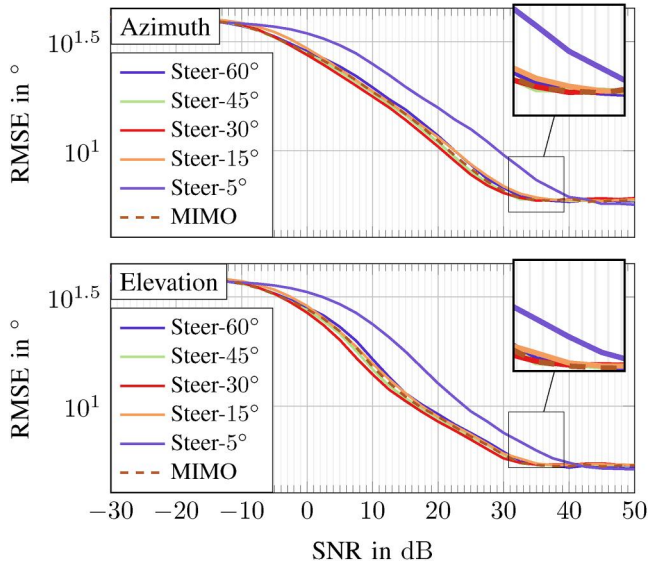


FIGURE 4 Direction of arrival (DoA) RMSE of a scenario with a single target. The employed radar system consists of a 2×2 transmit and a 2×2 receive antenna array.

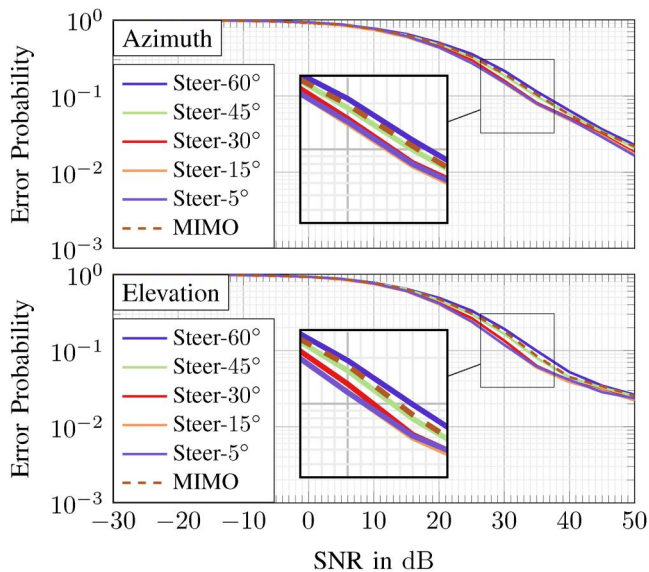


FIGURE 5 Direction of arrival (DoA) reconstruction error probability of a scenario with a single target. The employed radar system consists of a 2×2 transmit and a 2×2 receive antenna array.

signal processing of the MIMO mode at appropriate SNR. The DoA estimation improvement is in accordance with previous simulations for a single-dimension electronic beamsteering array [14]. This improvement of 2 dB–3 dB can even be extended by considering larger arrays, as those topologies offer narrower beams and thus enable a more precise electronic beamsteering.

Subsequently, an asymmetrically extended layout with $M_y \times M_z = 3 \times 5$ transmit and $N_y \times N_z = 5 \times 3$ receive elements is used as an example (cf. Figure 3b). These asymmetric arrays were deliberately chosen to show the effects of electronic beamsteering on the DoA estimate of a given angular dimension. In the MIMO processing mode, the array expands to a virtual aperture of 15×15 elements, which provides equal angular resolution in azimuth and elevation. The electronic beamsteering mode deals with square steering sets in the transmit domain with 25 steering directions and an accompanying asymmetrical receive array, which provides by itself a higher angular resolution in the elevation domain. An SNR penalty of $P_{\text{penalty}} = 2.2$ dB is applied to the electronic beamsteering receive signal. Looking at the RMSE curves in Figure 6, in azimuth dimension both array modes deliver basically similar results (with the exception of Steer-5°)—as with the former layout. The asymmetric layout of the receive array with a higher number of antenna elements in the y -direction benefits the elevation domain, which is reflected in a slight improvement of the RMSE based on the beamsteering compared to the MIMO mode. In general, all beamsteering ranges except Steer-5° and Steer-15° are well suited for DoA estimation, based on the RMSE. The resulting error probabilities are given in Figure 7 and show the impact of asymmetrically extended arrays on the performance. The electronic beamsteering can outperform the MIMO mode by up to 20% for DoA estimation in the elevation domain at an SNR of 15

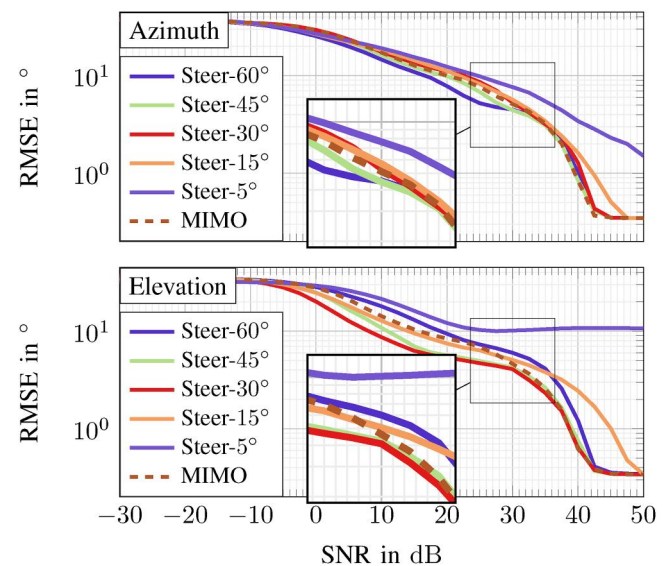


FIGURE 6 Direction of arrival (DoA) RMSE of a scenario with a single target. The employed radar system consists of a 3×5 transmit and a 5×3 receive antenna array.

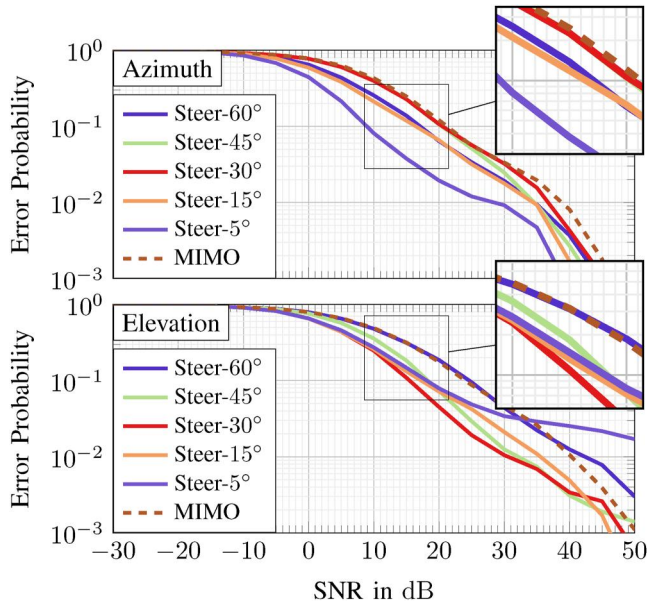


FIGURE 7 Direction of arrival (DoA) reconstruction error probability of a scenario with a single target. The employed radar system consists of a 3×5 transmit and a 5×3 receive antenna array.

dB, regardless of the chosen beamsteering range. In the azimuth domain, the improvement can be further extended when utilising a narrow electronic beamsteering range of $\pm 5^\circ$, which results in a reduction of the error probability by a factor of up to 5 at an SNR of 15 dB.

6 | DISCUSSION

The Grammian matrix $\mathbf{A}^T \mathbf{A}$ provides information regarding the coherency of the underlying columns of the sensing matrix \mathbf{A} . The ideal case would result in a perfectly orthogonal sensing matrix with its Grammian representation given by the identity matrix. CS relies on the incoherency of individual columns of the sensing matrix to determine the best approximate atom to a given underdetermined linear system of equations. This is usually measured by the mutual coherence which gives the largest inner product of any two column vectors of the sensing matrix [45]. Its maximum is reached with a value of *one* for two identical columns, and the minimum is defined by the Welch bound [46]. The Grammian matrix on the other hand paints a more complete picture of the coherency of each individual column pair in the sensing matrix. This can constitute a better numeric tool for estimating the resulting CS performance. For the presented second array layout with $M_y \times M_z = 3 \times 5$ transmit and $N_y \times N_z = 5 \times 3$ receive elements, the Grammian matrix of the sensing matrix for azimuth DoA estimation is shown in Figure 8, as well as for elevation estimation in Figure 9.

The simulation results in the previous section have shown that the electronic beamsteering phased array can improve in DoA estimation over a MIMO processing scheme regardless of the antenna array layout. Furthermore, the estimate

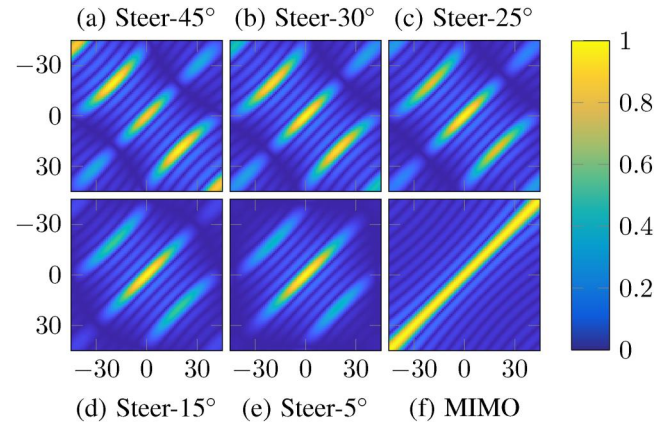


FIGURE 8 Normalised absolute Grammian matrices of the azimuth sensing matrix of the second exemplary radar system which consists of a 3×5 transmit and a 5×3 receive antenna array. The electronic beamsteering is performed in different sets with $L = 25$ discrete steering directions uniformly distributed in azimuth and elevation.

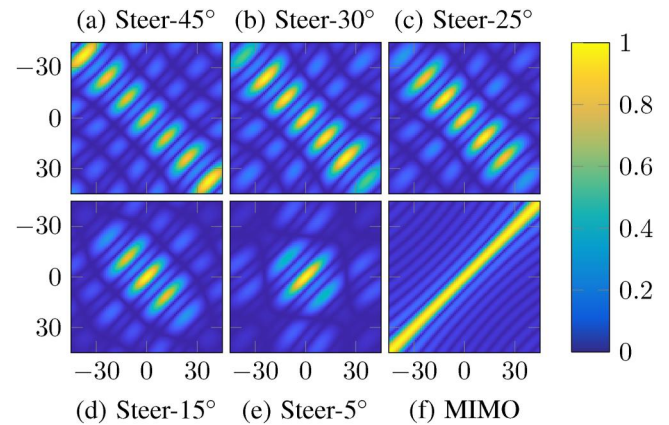


FIGURE 9 Normalised absolute Grammian matrix of the elevation sensing matrix of the second exemplary radar system which consists of a 3×5 transmit and a 5×3 receive antenna array. The electronic beamsteering is performed in different sets with $L = 25$ discrete steering directions uniformly distributed in azimuth and elevation.

improves when the estimation is performed for each angular domain separately. From the different steering sets illustrated in Figures 5 and 7, a relation between the improvement in reconstruction error probability and the chosen angular range for steering the main lobe of the antenna array becomes obvious. Correspondingly, a very narrow steering range seems to be advantageous for DoA estimation with an electronically steered array. However, the main beam of the array has to be sufficiently wide to still illuminate targets on the edges of the FoV. A similar technique is known as *sequential lobing* in radar tracking. This effect can be seen in the analysis of the smallest array in Figure 5, where the quality increases with a narrower electronic beamsteering range. As expected, this improvement holds for both angular dimensions of the DoA estimate.

In the second array layout in Figure 7, this statement holds only for the angular dimension with a larger number of elements in the transmit domain (given by the azimuth dimension

with $M_z = 5$). In this asymmetric case, the rectangular array affects the shape of the main lobe of the electronic beamsteering mode in the transmit domain. The rectangular receive array (rotated by 90°) leads to an improved angular resolution in the elevation domain compared to the azimuth domain. The simulation results show the effects of such an arrangement, since the receiving array is unable to reliably estimate the azimuth DoA for most ranges of electronic beamsteering. This is due to its coarser angular resolution. Improvement can be achieved for narrower beamsteering ranges. It only significantly outperforms the MIMO mode performance at a very narrow steering of $S_{\max} = 5^\circ$. From an antenna design perspective, these simulation results suggest optimising the electronic beamsteering based on both the layout of the transmit and receive arrays. Thus, narrower beamsteering in the area where the receive array provides the lower resolution appears advantageous. Additionally, a sharper main lobe of the transmit array (in the dimension with more antenna elements) may be steered in a broader steering range to illuminate the whole FoV.

Compared to the one-dimensional beamsteering presented in ref. [14], which leads to gains of about 3 dB compared to MIMO processing, a two-dimensional implementation provides significantly improved gains on the order of 10 dB for a single angular dimension. The RMSE curves of the simulations in Figures 4 and 6 show no significant improvement in mean angular resolution by electronic beamsteering compared to MIMO processing, with both processing methods remaining at the same level. However, comparing RMSE with the corresponding reconstruction error probability in Figures 5 and 7 shows that electronic beamsteering indeed leads to an improvement.

Considering these results from the perspective of the Grammian matrices shown in Figures 8 and 9, it seems desirable to construct the sensing matrix in such a way that the FoV is completely filled. The goal here is to avoid reoccurrence of the secondary maxima within the FoV. These can be recognised by new, broader maxima in the upper and lower regions next to the main diagonal. These have similar values as the main maxima on the main diagonal of the Grammian matrix.

This loose optimisation criterion would be described by a combination of the main lobe width and the steering set. In the presented case, the most promising beamsteering range for the elevation estimate should be between 25° and 15° , as can be seen in Figure 7 and in the changes between Figures 9c and d. Between these two beamsteering sets, new lobes begin to form on the outer diagonals of the Grammian matrix. In MIMO mode, the resulting virtual aperture is of square shape and thus presents equal DoA estimation resolutions in azimuth and elevation. This behaviour is clearly visible when comparing the dashed lines in Figure 7.

A strength of our considered design is that we employ a general antenna array topology, which allows for both conventional MIMO radar/virtual aperture processing and transmitter-sided beamsteering. Note that the beamsteering mode usually requires a larger number of time slots for a single DoA estimation than the MIMO mode. Correspondingly, in

highly dynamic target scenarios, it might still be useful to switch to the MIMO mode (at the expense of an inferior reconstruction error performance). A common array topology therefore allows for a seamless switching between both modes, in order to adapt the system to varying UAM requirements.

7 | CONCLUSION

UAM scenarios are highly dynamic and require fast and reliable information about the environment of an UAV for situational awareness. This paper introduced a framework for processing electronically steered radar data in terms of CS theory in order to provide accurate DoA estimation results with moderate receiver processing. In particular, a general antenna array topology was employed, which either allows for conventional MIMO radar/virtual aperture processing or transmitter-sided beamsteering. The simulative study has shown that the electronically steered MIMO array is capable to outperform the conventional MIMO mode DoA estimation performance when the electronic beamsteering set is chosen appropriately based on the intended angular domain and the underlying antenna array layout. From a radar array design perspective, the presented arrays have been chosen rather conservatively as URAs. When using electronic beamsteering, optimisation must be based on the respective merits of each antenna array: Narrow beamsteering can be used in the angular dimension where the transmit array can provide good angular resolution (e.g. where the larger number of antenna elements are placed) and the receive array has fewer elements and thus provides coarser angular resolution. At the same time, a beamsteering mode optimised on the Grammian representation of the sensing matrix can be employed in the angular domain where the receiving array provides the larger number of antenna elements and thus higher resolution. It can be concluded that the percentage of correct reconstructions is significantly higher for the electronic beamsteering mode than for the conventional orthogonal signal-based MIMO mode. While incorrect DoA reconstructions of either mode do not have significant impact on the resulting RMSE performance (both modes offer a comparable RMSE performance), our numerical results have shown that the reconstruction error probability can be significantly reduced by means of the electronic beamsteering mode without sacrificing RMSE performance—which is important, as both metrics are relevant.

Besides the improvement of the estimation via separated processing in azimuth and elevation, the numerical simulations suggest a key factor for improved estimation performance in the selection of beamsteering directions. In this study, a variety of different beamsteering sets has been investigated, influenced by the overall steering range in azimuth or elevation.

So far, our proposed beamsteering schemes employ only a single beam direction at a time. Yet, by superimposing weight vectors, multiple simultaneous beam directions would also be feasible, which potentially offers further advantages. Corresponding extensions of our beamsteering schemes are thus an interesting direction for future work.

AUTHOR CONTRIBUTIONS

Max Schurwanz: Conceptualisation; Data curation; Formal analysis; Investigation; Methodology; Software; Validation; Visualisation; Writing – original draft; Writing – review & editing.

Jan Mietzner: Conceptualisation; Formal analysis; Funding acquisition; Investigation; Methodology; Project administration; Resources; Supervision; Writing – review & editing.

Peter Adam Hoehner: Formal analysis; Funding acquisition; Methodology; Supervision; Writing – review & editing.

ACKNOWLEDGEMENTS

Reported research was supported by the project Master360 funded by the German Federal Ministry for Economic Affairs and Climate Action (BMWK) under grant number 20D1905B.

Open Access funding enabled and organized by Projekt DEAL.

CONFLICT OF INTEREST STATEMENT

The authors declare no conflict of interest.

ETHICS APPROVAL STATEMENT

Not applicable.

PATIENT CONSENT STATEMENT

Not applicable.

PERMISSION TO REPRODUCE MATERIAL FROM OTHER SOURCES

Not applicable.

CLINICAL TRIAL REGISTRATION

Not applicable.

DATA AVAILABILITY STATEMENT

Research data are not shared.

ORCID

Max Schurwanz  <https://orcid.org/0000-0002-4557-744X>

Jan Mietzner  <https://orcid.org/0000-0001-9084-9443>

Peter Adam Hoehner  <https://orcid.org/0000-0003-3475-1710>

REFERENCES

- Richards, M.A., Scheer, J.A., Holm, W.A.: Principles of Modern Radar. SciTech Publishing (2010)
- Bauranov, A., Rakas, J.: Designing airspace for urban air mobility: a review of concepts and approaches. Prog. Aero. Sci. 125, 100726 (2021). <https://doi.org/10.1016/j.paerosci.2021.100726>
- Johannsen, N.L., et al.: Joint Communication, Sensing and Localization for Airborne Applications (2022). <https://doi.org/10.48550/ARXIV.2209.10991>
- Fishler, E., et al.: MIMO radar: an idea whose time has come. In: Proc. 2004 IEEE Radar Conference, pp. 71–78 (2004)
- Li, J., Stoica, P.: MIMO radar with colocated antennas. IEEE Signal Process. Mag. 24(5), 106–114 (2007). <https://doi.org/10.1109/MSP.2007.904812>
- Miralles, E., et al.: Multifunctional and compact 3D FMCW MIMO radar system with rectangular array for medium-range applications. IEEE Aero. Electron. Syst. Mag. 33(4), 46–54 (2018). <https://doi.org/10.1109/MAES.2018.160277>
- Haimovich, A.M., Blum, R.S., Cimini, L.J.: MIMO radar with widely separated antennas. IEEE Signal Process. Mag. 25(January), 116–129 (2008). <https://doi.org/10.1109/msp.2008.4408448>
- Nickel, U.: Fundamentals of signal processing for phased array radar. Advanced Radar Systems, Signal and Data Processing, 1–22 (2006)
- Mailloux, R.J.: Phased Array Antenna Handbook. Artech House (2018). <https://doi.org/10.1108/sr.1999.08719bae.004>
- San Antonio, G., Fuhrmann, D.: Beampattern synthesis for wideband MIMO radar systems. In: 1st IEEE International Workshop on Computational Advances in Multi-Sensor Adaptive Processing, 2005, pp. 105–118 (2005). <https://doi.org/10.1109/CAMAP.2005.1574195>
- He, H., Stoica, P., Li, J.: Wideband MIMO systems: signal design for transmit beampattern synthesis. IEEE Trans. Signal Process. 59(2), 618–628 (2011). <https://doi.org/10.1109/TSP.2010.2091410>
- Deligiannis, A., Chambers, J.A., Lambotaran, S.: Transmit beamforming design for two-dimensional phased-MIMO radar with fully-overlapped subarrays. In: 2014 Sensor Signal Processing for Defence (SSPD 2014), pp. 6–9 (2014). <https://doi.org/10.1109/SSPD.2014.6943318>
- Morency, M.W., Vorobyov, S.A.: Partially adaptive transmit beamforming for search free 2D DOA estimation in MIMO radar. In: 2015 23rd European Signal Processing Conference (EUSIPCO 2015), pp. 2631–2635 (2015). <https://doi.org/10.1109/EUSIPCO.2015.7362861>
- Schurwanz, M., Mietzner, J., Hoehner, P.A.: Compressive sensing for direction-of-arrival estimation using an electronically steered multiple-input multiple-output array. In: 2021 18th European Radar Conference (EuRAD), pp. 401–404 (2021)
- Schwarz, D., et al.: Improving the detection capability of imaging MIMO radars by tx beamforming. In: 2022 25th European Microwave Week (EuMW), pp. 17–20 (2022)
- Fuhrmann, D.R., Antonio, G.S.: Transmit beamforming for MIMO radar systems using signal cross-correlation. IEEE Trans. Aero. Electron. Syst. 44(1), 171–186 (2008). <https://doi.org/10.1109/TAES.2008.4516997>
- Hassanien, A., Vorobyov, S.A.: Phased-MIMO radar: a tradeoff between phased-array and MIMO radars. IEEE Trans. Signal Process. 58(6), 3137–3151 (2010). <https://doi.org/10.1109/TSP.2010.2043976>
- Li, H., Himed, B.: Transmit subaperturing for MIMO radars with Co-located antennas. IEEE Journal of Selected Topics in Signal Processing 4(1), 55–65 (2010). <https://doi.org/10.1109/JSTSP.2009.2038967>
- Hassanien, A., Vorobyov, S.A.: Transmit energy focusing for DOA estimation in MIMO radar with colocated antennas. IEEE Trans. Signal Process. 59(6), 2669–2682 (2011). <https://doi.org/10.1109/TSP.2011.2125960>
- Hassanien, A., et al.: Two-dimensional transmit beamforming for MIMO radar with sparse symmetric arrays. In: Proc. IEEE National Radar Conference (2013). <https://doi.org/10.1109/RADAR.2013.6586078>
- Trees, H.L.V.: Optimum Array Processing. John Wiley & Sons, Inc. (2002)
- Li, J., Stoica, P.: MIMO Radar Signal Processing. Wiley Online Library (2009)
- Schmidt, R.: Multiple emitter location and signal parameter estimation. IEEE Trans. Antenn. Propag. 34(3), 276–280 (1986). <https://doi.org/10.1109/tap.1986.1143830>
- Roy, R., Kailath, T.: ESPRIT-estimation of signal parameters via rotational invariance techniques. IEEE Trans. Acoust. Speech Signal Process. 37(7), 984–995 (1989). <https://doi.org/10.1109/29.32276>
- Krim, H., Viberg, M.: Two decades of array signal processing research. IEEE Signal Process. Mag. 13(4), 67–94 (1996). <https://doi.org/10.1109/79.526899>
- Candès, E.J., Tao, T.: Near-optimal signal recovery from random projections: universal encoding strategies? IEEE Trans. Inf. Theor. 52(12), 5406–5425 (2006). <https://doi.org/10.1109/tit.2006.885507>
- Candès, E.J., Romberg, J., Tao, T.: Robust uncertainty principles: exact signal reconstruction from highly incomplete frequency information. IEEE Trans. Inf. Theor. 52(2), 489–509 (2006). <https://doi.org/10.1109/tit.2005.862083>

28. Yu, Y., Petropulu, A.P., Poor, H.V.: Compressive sensing for MIMO radar. In: 2009 IEEE Int. Conf. Acoustics, Speech and Signal Processing, pp. 3017–3020 (2009). <https://doi.org/10.1109/ICASSP.2009.4960259>
29. Abdul, M., et al.: Compressive sensing applied to radar systems: an overview. *Signal, Image and Video Processing* 9(1), 25–39 (2015). <https://doi.org/10.1007/s11760-015-0824-y>
30. Abo-Zahhad, M.M., Hussein, A.I., Mohamed, A.M.: Compressive sensing algorithms for signal processing applications: a survey. *Int. J. Commun. Netw. Syst. Sci.* 8(05), 197–216 (2015). <https://doi.org/10.4236/ijcns.2015.85021>
31. Stahl, H., et al.: Sub-Nyquist radar with optimized sensing matrices — performance evaluation based on simulations and measurements. In: 2016 4th Int. Workshop on Compressed Sensing Theory and its Applications to Radar, Sonar and Remote Sensing (CoSeRa), pp. 242–246 (2016). <https://doi.org/10.1109/CoSeRa.2016.7745737>
32. Rossi, M., Haimovich, A.M., Eldar, Y.C.: Spatial compressive sensing for MIMO radar. *IEEE Trans. Signal Process.* 62(2), 419–430 (2014). <https://doi.org/10.1109/TSP.2013.2289875>
33. Schurwanz, M., et al.: Compressed sensing based obstacle detection for future urban air mobility scenarios. *IEEE Sensors Letters* 7(11), 1–4 (2023). <https://doi.org/10.1109/LENS.2023.3323867>
34. Harlakin, A., et al.: Compressive-sensing-aided MIMO radar enabling multi-functional and compact sensors in air scenarios using optimized antenna arrays. *IEEE Access* 9, 41417–41429 (2021). <https://doi.org/10.1109/ACCESS.2021.3065214>
35. Rogers, C.A., Popescu, D.C.: Compressed sensing MIMO radar system for extended target detection. *IEEE Syst. J.* 15(1), 1381–1389 (2020). <https://doi.org/10.1109/jsyst.2020.3000500>
36. Schurwanz, M., et al.: Compressive sensing techniques applied to a semi-circular mmWave MIMO array. In: 2023 22th International Radar Symposium (IRS), pp. 1–10 (2023)
37. Chen, P., Zhan, P., Wu, L.: Clutter estimation based on compressed sensing in bistatic MIMO radar. In: 2017 Int. Conf. Communication, Control, Computing and Electronics Engineering (ICCCCEE), pp. 1–6 (2017). <https://doi.org/10.1109/ICCCCEE.2017.7867639>
38. Schurwanz, M., et al.: Using widely separated MIMO antennas for UAV radar direction-of-arrival estimation. In: 2022 19th European Radar Conference (EuRAD), pp. 281–284 (2022)
39. Gu, Y., Zhang, Y.D., Goodman, N.A.: Optimized compressive sensing-based direction-of-arrival estimation in massive MIMO. In: 2017 IEEE International Conference on Acoustics, Speech and Signal Processing (ICASSP), pp. 3181–3185. IEEE (2017)
40. Guo, M., Zhang, Y.D., Chen, T.: DOA estimation using compressed sparse array. *IEEE Trans. Signal Process.* 66(15), 4133–4146 (2018). <https://doi.org/10.1109/tsp.2018.2847645>
41. Wen, F., et al.: Compressive sampling framework for 2D-DOA and polarization estimation in mmWave polarized massive MIMO systems. *IEEE Trans. Wireless Commun.* 22(5), 3071–3083 (2022). <https://doi.org/10.1109/twc.2022.3215965>
42. Hassanien, A., Vorobyov, S.A.: Transmit/receive beamforming for MIMO radar with colocated antennas. In: 2009 IEEE International Conference on Acoustics, Speech and Signal Processing, pp. 2089–2092 (2009). <https://doi.org/10.1109/ICASSP.2009.4960027>
43. Blumensath, T., Davies, M.E.: Iterative thresholding for sparse approximations. *J. Fourier Anal. Appl.* 14(5-6), 629–654 (2008). <https://doi.org/10.1007/s00041-008-9035-z>
44. Cai, T.T., Wang, L.: Orthogonal matching pursuit for sparse signal recovery with noise. *IEEE Trans. Inf. Theor.* 57(7), 4680–4688 (2011). <https://doi.org/10.1109/TIT.2011.2146090>
45. Donoho, D.L., Elad, M.: Optimally sparse representation in general (nonorthogonal) dictionaries via ℓ_1 minimization. *Proc. Natl. Acad. Sci. USA* 100(5), 2197–2202 (2003). <https://doi.org/10.1073/pnas.0437847100>
46. Kutyniok, G.: Compressed sensing. *Mitteilungen der Deutschen Mathematiker-Vereinigung* 22(1), 24–29 (2014). <https://doi.org/10.1515/dmvm-2014-0014>

How to cite this article: Schurwanz, M., Mietzner, J., Hoehner, P.A.: Improving estimation performance of compressive sensing-based multiple-input multiple-output radar using electronic beamsteering. *IET Radar Sonar Navig.* 18(6), 891–903 (2024). <https://doi.org/10.1049/rsn2.12535>